J MATER SCI **41** (2006) 4061–4073

Experimental determination of the thermal conductivity of three-phase syntactic foams

V. S. SHABDE, K. A. HOO*
Department of Chemical Engineering, Texas Tech University, Lubbock, TX 79409-3121
E-mail: karlene.hoo@ttu.edu

G. M. GLADYSZ
Los Alamos National Laboratories, Los Alamos, NM 87545

Published online: 7 June 2006

Syntactic foams are attractive for applications that require materials with high impact strength and low thermal conductivities. Because syntactic foams are manufactured by dispersing hollow microspheres in a resinous matrix, their characteristics are functions of the type and relative amounts of these materials. In this work, a discussion of an experimental approach to measure the thermal conductivity of three-phase syntactic foams (hollow carbon microspheres in a porous APO-BMI binder, analysis of the data and the comparison to predictive models are presented. The thermal conductivity of three-phase syntactic foams is measured using a Holometrix© steady-state heat flow meter. The experimental data are found to be accurate to within a reasonable range of experimental error and are compared to three of the more reliable predictive models that have been used successfully to estimate the thermal conductivity of similar foams. It is observed that the model predictions at lower temperatures are more accurate as compared to those at higher temperatures. Also, that a model based on the concept of self-consistent field theory better predicts the thermal conductivity of syntactic foams than one based on resistance-in-series. Sensitivity studies indicate a strong dependency of the thermal conductivity of the three-phase foams on the thermal conductivity of the carbon used in the microspheres.

1. Introduction

Plastic foams are lightweight materials consisting of at least two phases, a solid polymer phase and a gaseous phase. The presence of the gaseous phase provides the foam with certain desirable characteristics such as low density and low thermal conductivity, while the polymeric phase provides structure to the foam. To further enhance the thermo-physical properties of the foam a third hollow material is added, which gives rise to the class of three-phase composite foams. Syntactic foams are a special class of composite foams and consist of hollow microspheres, called fillers, in a resinous matrix, called the binder [1]. Microspheres may be made from polymers, ceramics, or metals. The matrix material may be thermosetting resins such as epoxy resins, polyimide resins, asphalt, or thermoplastic resins such as polyethylene [1].

This work focuses on three-phase syntactic foams that are composed of hollow carbon microspheres as the filler, APO-bismaleimide (APO-BMI) (Honeywell FM&T, Kansas City, MO) resin as the binder and air-voids within the binder matrix as the third phase. Since the microspheres and air-voids are distributed randomly throughout the polymer matrix, the thermo-physical properties are independent of the orientation of the foam (isotropic).

A number of techniques are available to measure thermal conductivity of different materials. These techniques are classified as stationary or non-stationary. The stationary methods that employ a guarded heat flow meter are the most popular methods to measure thermal conductivity of low conductivity materials [2]. The specific experimental apparatus used in this work is a Holometrix© TCA-200LT-A guarded heat flow meter [3]. The range

*Author to whom all correspondence should be addressed.
0022-2461
DOI: 10.1007/s10853-006-7637-x

of temperatures that is investigated is between 273 K and 473 K.

For heterogenous materials, the concept of a *pure* thermal conductivity is not realistic. However, when conduction is the main source of heat transfer, an *effective* thermal conductivity may be defined [4–8]. The effective thermal conductivity represents the ratio of the heat transferred across a bulk sample of the material under consideration to the temperature difference across the sample. In foams, apart from conduction, radiation and convection may also occur due to the presence of the gas phase. These phenomena also need to be considered when estimating an effective thermal conductivity. Thus a knowledge of the exact mode of heat transfer in the foams is necessary for modeling thermal conductivity in foams. In general, heat transfer in foams is more complex due to the presence of the gas phase. A large volume of work has been done on modeling the thermal conductivity of solid composites. One of the simplest models is the series/parallel model based on the analogy of thermal resistance to electrical resistance [4]. Agari and Uno [10] modified the series/parallel model to account for the arrangement of the filler in the matrix. Their predictions are quite accurate for graphite filled composites [10]. Cheng and Vachon proposed a model based on the electrical resistance analogy. In their work, they assume that the geometric shape of the discontinuous phase in the sample is described by a parabola [11]. Maxwell [12] proposed *self-consistent field* theory to estimate properties of composite materials. The use of this theory is found to be accurate for two-phase systems in which one phase is present in a very small amount. Hashin [7] and Benveniste [8] have developed models for two-phase composites based on theory of a self-consistent field. Felske [6] extended the self-consistent field theory model to two-phase syntactic foams.

At low temperatures, heat transfer due to radiation in foams is negligible but at moderate to large temperatures, the contribution to heat flow due to thermal radiation is not insignificant; this effect affects the accuracy of the prediction of the thermal conductivity especially in the case of highly porous *open-celled* foams [13]. Others [4, 5, 14, 15] have modeled the contribution due to radiation as a diffusive process. Contribution to heat transfer due to convection is very small in foams.

Models of the effective thermal conductivity of three-phase foams are not available in the open literature. This work introduces a procedure to model the effective thermal conductivity of three-phase foams by calculating an equivalent thermal conductivity for the microspheres phase, and one for the combined binder and filler phases. The final effective thermal conductivity of the foam is calculated using the predictive models of Cheng and Vachon, Eucken, and Leach.

The paper is organized as follows. Section 2 describes the experimental setup of the Holometrix© TCA-200LT-A guarded heat flow meter. Section 3 introduces three existing models to predict the thermal conductivity of foams. Section 4 presents the experimental data and compares the experimental thermal conductivity to the predictions of the models. Lastly, Section 5 summarizes the results and identifies future work.

2. Measuring the thermal conductivity

The experimental methods to measure thermal conductivity are classified as either stationary or non-stationary methods. The basic difference is that the former method requires the sample to be at a stationary state. Guarded, one-specimen, or two-specimen flow meters are stationary methods while hot-wire, flash radiometry, and transient plane source methods are non-stationary methods. Both stationary and non-stationary methods have been used to measure the thermal conductivity of foams [16–20].

This work employs the principles of a stationary guarded heat flow meter to measure the thermal conductivity of three-phase syntactic foams. In the heat flow meter, a sample of the material whose thermal conductivity is to be measured is placed between two conducting plates and a constant temperature difference is applied across the sample. If the heat flux across the sample and the temperature difference are measured then the thermal conductivity can be determined.

2.1. Experimental approach

A number of techniques are available to measure thermal conductivity of different materials. These techniques are classified as stationary or non-stationary. Some examples of non-stationary techniques include: 1) Flash radiometry and 2) the Hot-wire method. In flash radiometry, physical properties such as the thermal diffusivity and specific heat capacity of the material are required. Since these properties are not known a priori for the samples used in this work, flash radiometry cannot be used. The hot-wire technique is based on measuring the temperature rise of a sample across which an electrically heated wire is passed. This wire acts as a line heat source to the sample. The change in temperature with time is used to calculate the thermal conductivity [21]. While this technique is suitable for measuring low thermal conductivity, accuracy becomes an issue when large temperature gradients are present. In addition, tests by Davis [21] have shown that the hot-wire method may be very inaccurate since a constant heat output over the length of the wire is assumed.

2.2. The guarded heat flow meter

The guarded heat flow meter technique is based on Fourier's law of heat conduction [2]. Fourier's law states that the rate of heat conduction through a material is

directly proportional to the temperature gradient across the material. Consider a material with two opposite planar surfaces at temperatures, T_1 and T_2, respectively, with $T_2 > T_1$. The second law of thermodynamics tells us that heat flows from surface at temperature T_2 to the surface at temperature T_1. Then, the rate of heat conduction, q, across the two surfaces is given by,

$$q = -k\frac{dT}{dz} = -k\frac{(T_1 - T_2)}{z}, \tag{1}$$

where q is the heat flux across the sample in W m^{-2}, k is the thermal conductivity with units of $W\,m^{-1}K^{-1}$, ΔT is the temperature difference across the sample in degrees Kelvin, and z is the distance in meters between surfaces 1 and 2.

Another quantity which is useful is the thermal resistance, R_s, of the sample. It is defined as a ratio of the distance between the two plates to the thermal conductivity [2] ,

$$R_s \equiv \frac{z}{k} = \frac{T_2 - T_1}{q} \tag{2}$$

The thermal resistance has units of m^2 K W^{-1}.

In a guarded heat flow meter, a sample of the material whose thermal conductivity is to be measured is placed between two conducting plates and a constant temperature difference is applied across the sample. The temperatures of both plates are controlled by a differential controller. Using the above two equations, the thermal conductivity at different temperatures can be calculated.

Since, by definition, composite materials consist of at least two distinct materials, thermal conductivity of composite materials is a function of the thermal conductivities of its individual constituents. Moreover, the thermal conductivity of composite materials is also dependent on the internal structure, i.e. the position and alignment of the individual constituents. Therefore, for composite materials, such as foams, the concept of a thermal conductivity is not valid. However, the concept of an *equivalent thermal conductivity* for the material may be used if the mechanism for heat transfer is mainly conduction. In such a case, however, the thermal resistance defined in Equation 2 is some non-linear function of ΔT and q, that is determined experimentally.

Initially, the guarded heat flow meter is calibrated using samples whose thermal conductivities are known at different temperatures. From the known values of the thermal conductivities, the thermal resistances can be found. When the samples are actually tested, knowing the ratio of the temperature difference across the sample to heat flow permits the sample resistance to be estimated from the calibration and in-turn the thermal conductivity can be calculated.

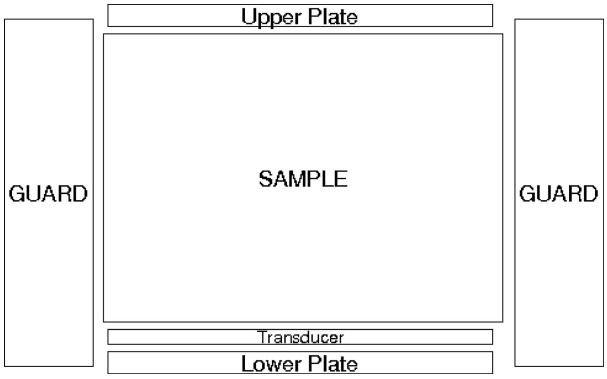

Figure 1 A schematic of the test section in the Holometrix© TCA-200LT-A guarded heat flow meter.

2.3. Experimental procedure

The thermal conductivity analyzer consists of a cylindrical test section with two parts [3] a schematic of which is shown in Fig. 1. The upper part can be moved pneumatically but the lower part is fixed. The sample is placed in the sample holder inside the lower part. The recommended pressure to the upper part is about 500 kPa. The upper part includes a heat sink separated by insulation from a copper plate. The copper plate is heated electrically and acts as the upper plate heater. Thermocouples are provided to measure the temperature of the sample and the temperature of the lower copper plate. The lower part also has a copper plate, which acts as the lower plate heater. The lower plate heater is maintained at about 298 K higher temperature than the upper plate heater while a temperature difference of 30 K is maintained across the sample, Thus, the direction of heat flow is upwards. There is a heat flux transducer to measure the heat transferred to the sample. A cylindrical guard heater surrounds the sample assembly. The guard heater is maintained at a temperature close to the mean sample temperature to avoid radial heat losses. There are heat sinks below the lower plate and around the sample. A 50% by volume solution of ethylene-glycol and water is circulated through the heat sinks to maintain the temperatures.

The accuracy of the water bath that controls the temperature of the ethylene glycol-water mixture is 1 K. This is especially important for low temperature experiments. Moisture that condenses on the test surfaces during the experiment may distort the results. To prevent this, an inverted bell jar is placed over the test section isolating it from the ambient conditions. This chamber is filled with an inert, dry gas such as nitrogen or argon to prevent moisture from forming inside the chamber. The thermocouple temperature measurements are automatically collected and stored in a dedicated computer.

The heat flow meter is calibrated using samples provided by Holometrix©. The calibration samples are 0.0125 m thick Pyrex, 0.00625 m thick Pyrex, and 0.0125 m thick Vespel. The thermal conductivities of

these materials are known. These samples are individually placed in the sample holder and tested at the desired range of temperatures, which in this project, are between 273 K and 473 K in increments of 25 K. Based on the measurements, the system is calibrated using calculated values of the sample resistance that are a function of the temperature difference across the sample and the heat flux through the sample.

Once the calibration file has been generated, the sample is tested. The sample has a diameter of about 50 mm and thickness of about 6 to 6.5 mm. The sample is coated with a Dow-Corning heat sink compound to prevent heat losses where the sample touches the upper and lower plates. The sample is tested over the same temperature range in which the calibration was made.

Analysis of the test data requires that the sample resistance be determined by comparing the data collected during the experiment to the data obtained during calibration. Knowing the thermal conductivities of the calibration samples at different temperatures, a relationship can be established between the thermal resistance and the ratio of the temperature difference across the sample and the heat flux through it, which in turn can be used to calculate the thermal resistance of the test sample. The thermal conductivity can then be calculated from the thermal resistance using Equation 2.

3. Thermal conductivity models

For heterogenous materials such as foams, the thermal conductivity is an average property of a sample, or an *effective thermal conductivity*. Thus, the thermal conductivity is a function of not only the temperature of the material but also the properties of the sample, specifically, the density of the sample. Any mathematical model to estimate the thermal conductivity of foams must relate the density of the foam to the thermal conductivity. In addition, if the foam is highly porous, radiative heat transfer effects must be accounted for.

3.1. Heat transfer in foams

Heat transfer through foams may occur due to a combination of conduction, radiation, and convection. The conductive heat transfer is the most dominant while convective heat transfer is usually negligible except in the case of highly porous foams [13]. In the present work, heat transfer due to convection is neglected.

The primary mechanism for heat transfer through foams is conduction. Conduction takes place through the solid and gaseous phases. Since the thermal conductivity of the gaseous phase is low ($\sim$0.029 W m^{-1}K^{-1} at 298 K), the gaseous phase provides the maximum resistance to heat flow due to conduction. Most of the models for thermal conductivity of composites are conduction models [4].

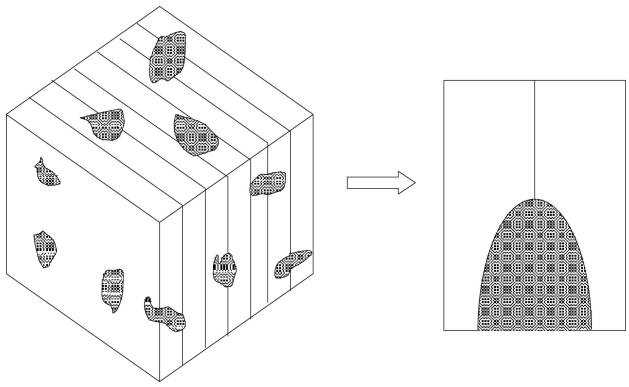

Figure 2 Illustration of the rearrangement of the discontinuous phase in the Cheng-Vachon series model.

In porous materials, particularly those with a large percentage of voids, radiative heat transfer plays an important role [5, 13]. Thus, any model to estimate the thermal conductivity of these materials cannot neglect the contribution due to radiation. Radiative heat transfer may be modeled as a diffusive process if the optical thickness, τ_0 is large ($>$2). The optical thickness can be calculated from the actual thickness, t, and the extinction coefficient, β (the fraction of incident radiation which is scattered or absorbed [22]). That is,

$$\tau_0 \equiv \beta_t$$

where t is in meters, and β has units of m^{-1} Foams are generally optically thick [4] . In this work, the radiative heat transfer is modeled as a diffusive process using the Rosseland equation [22].

3.2. Conductive heat transfer

An overview of three of the more common models that can be used to estimate the effective thermal conductivity by conductive heat transfer are presented. The first model, called Cheng-Vachon model [11] assumes a normal distribution of the discontinuous phase in the foam. The other model, contributed by Eucken [23], is based on *self-consistent field theory*.

3.2.1. Resistances in series model

Cheng and Vachon [11] propose a model for thermal conductivity using the analogy between heat flow and electrical flow. They modeled the discontinuous phase in the composite as a parabolic function. Then, a unit cell of the composite is sectioned into differential elements that are perpendicular to the direction of heat flow. Assuming that heat flows perpendicular to the differential elements, a relationship is developed that is based on the selected geometry. In this work, the Cheng-Vachon model used to estimate the effective thermal conductivity is given by

[11],

$$k_{\text{eff}} = R_e^{-1} = \frac{2}{\sqrt{C(k_d - k_c)}} \times \arctan\left(\frac{B}{2}\sqrt{\frac{C(k_d - k_c)}{k_c + B(k_d - k_c)}}\right) + \frac{1 - B}{k_c} \quad (3)$$

$$B = \sqrt{\frac{3v_d}{2}}; \qquad C = \frac{4}{B}$$

where k_{eff} is the effective thermal conductivity of the foam, R_e is the thermal resistance per unit thickness of the sample, k_{solid} is the thermal conductivity of the solid phase, k_d is the thermal conductivity of the discontinuous phase, v_d is the volume fraction of the discontinuous phase, and C and B are parameters that are a function of v_d.

3.2.2. Self consistent field theory

A large amount of the research on modeling of composites has focused on the use of *self-consistent field* theory. Self-consistent field theory can be used to determine the effective thermal conductivity of the composite provided the individual pure thermal conductivities are known. A brief overview, taken from [6, 7], is provided as this work requires an understanding of this theory.

Consider a sample of a composite material suspended in a homogenous medium having the same thermal conductivity as the composite. Then, imposing the same temperature difference across the composite and the homogenous medium the effective thermal conductivity is calculated as the ratio of the average heat flow to the average temperature gradient across the composite. For a temperature gradient applied to a composite, the heat flux flowing through the composite, based on self-consistent field theory, is given by,

$$q = k_{\text{eff}} \nabla T \quad (4)$$

where q is the heat flux, ∇T is the temperature gradient, and k_{eff} is the effective thermal conductivity of the medium. This approach has been used to determine other effective properties for instance, an effective electrical conductivity and an effective magnetic permeability [7]. Hashin's equation can be used to determine the effective thermal conductivity of the hollow carbon microspheres [7],

$$k_{\text{cmb}} = k_c \left(1 + \frac{v_a}{\frac{k_c}{k_c - k_a} + \frac{v_a}{3}}\right) \quad (5)$$

where k_{cmb} is the effective thermal conductivity, k_c is the thermal conductivity of the carbon in the wall of the microsphere, k_a is the thermal conductivity of air, and v_a is the volume fraction of air in the microsphere.

Maxwell's relationship based on the assumption of a unidirectional heat flow can be used to determine the effective thermal conductivity of the binder *and* microsphere phases [12],

$$k_{\text{solid}} = k_{\text{cmb}} \frac{k_{\text{binder}} + 2k_{\text{cmb}} - 2v_{\text{binder}}(k_{\text{cmb}} - k_{\text{binder}})}{k_{\text{binder}} + 2k_{\text{cmb}} + v_{\text{binder}}(k_{\text{cmb}} - k_{\text{binder}})}. \quad (6)$$

Note that this equation uses the result of Equation 5.

Eucken proposes the following model to estimate the effective thermal conductivity of porous materials [23],

$$k_{\text{eff}} = k_{\text{solid}} \left(\frac{1 + 2v_a\left(\frac{1-Q_1}{1+2Q_1}\right)}{1 - v_a\left(\frac{1-Q_1}{1+2Q_1}\right)}\right) \quad (7)$$

where

$$Q_1 = \frac{k_{\text{solid}}}{k_a}$$

and the meaning of the variables are unchanged.

In the case of low density two-phase foams, Leach provides the following expression [4],

$$k_{\text{eff}} = k_{\text{air}} + \frac{2}{3}\left(\frac{\rho_{\text{foam}}}{\rho_{\text{solid}}}\right) k_{\text{solid}} \quad (8)$$

3.3. Radiative heat transfer

The models presented in Section 3.2 do not account for radiative heat transfer, which in the case of porous materials may be almost as important as conductive heat transfer. In this work, the Rosseland equation [15] will be used to model the heat transfer due to radiation.

Heat transfer due to radiation is attributed to the emission of photons. When a photon is emitted, its motion may cause it to strike another particle and then become scattered. Inside a foam, the part that is at a higher temperature emits photons that strike the surface of other parts of the foam and scatter. If the mean free path of the photons between collisions is much smaller compared to the dimensions of the foam, the mechanism of heat transfer can be modeled as a diffusion process [15]. The radiative heat transfer can then be calculated as follows [15, 22],

$$q_r = \frac{16\sigma T^3}{3\beta}\left(\frac{\partial T}{\partial x}\right) \quad (9)$$

where q_r is the radiative heat flux, β is the extinction coefficient which is the reciprocal of the mean free path, T is temperature, x is the distance from the heat source, and

σ is the Stefan-Boltzmann constant. The only unknown in the above equation is the extinction coefficient. The extinction coefficient may be determined experimentally by using Fourier Transform Infra-Red (FTIR) spectroscopy for open cell foams [16]. Glicksman also provides a model for the extinction coefficient for closed cell foams based on the structure of the cell wall [5]. In the current work, since the interstitial voids are interconnected they cannot be treated as closed cell foams. Hence, a suitable open cell model developed by Wei [16] is used.

$$\beta = 42.038\rho_f + 121.55 \tag{10}$$

where ρ_f is the density of the foam in kg m^{-3}, and β is the extinction coefficient in cm^{-1}. Suppose that the radiative thermal conductivity, k_r, can be defined in a similar manner as pure conductivity. That is,

$$q_r = k_r \frac{\partial T}{\partial x}, \tag{11}$$

Substitution of Equations 9 and 11 and rearrangement give the radiative thermal conductivity as,

$$k_r = \frac{16\sigma T^3}{3\beta} \tag{12}$$

To summarize, the approach used in this work to represent heat transfer due to conduction and radiation is as follows:

1. In the case of heat conduction, *self-consistent field* theory is applied [7, 12]. The microsphere wall is assumed to be the matrix and the trapped air is assumed to be the spheroidal inclusion. Equation 5 for a sphere inside a matrix may be used [7] to determine the thermal conductivity of the carbon microspheres.
2. The effective thermal conductivity of the solid material (binder and filler) is calculated assuming there is no air present. Equation 6 is applied since the amount of binder in the samples is very small.
3. Once the thermal conductivity of the solid (filler and binder) is determined the foam is treated as a two-phase material and the effective thermal conductivity of this pseudo-two-phase material is determined using three different approaches, series-parallel model Equation 3, self-consistent theory Equation 7 and Equation 8, which is most commonly used to estimate the thermal conductivity of two-phase foams with high porosity.

Suppose q is the conductive heat flow through the sample and q_r is the radiative heat flow. Then the total flow q_{tot} across the sample is,

$$\begin{aligned} q_{\text{tot}} &= q + q_r \\ q_{\text{tot}} &= k_{\text{tot}} \frac{\partial T}{\partial x} \\ k_{\text{tot}} \frac{\partial T}{\partial x} &= k_{\text{eff}} \frac{\partial T}{\partial x} + k_r \frac{\partial T}{\partial x} \\ k_{\text{tot}} &= k_{\text{eff}} + k_r \end{aligned}$$

Thus, the radiative and conductive thermal conductivities can be added to obtain the overall effective thermal conductivity [13]. The contribution of the heat transferred due to radiation is calculated using Equation 12.

4. Results and discussion

4.1. Statistical analysis

Real data always contain some error. To determine the range of the errors in the experimental data, an uncertainty analysis is carried out [24]. The uncertainty in the error is found to be approximately, $\pm 3\%$ (Appendix B). The samples are composed of different densities of the carbon microspheres and different volume fractions of carbon in the foams (see Table III of Appendix A). Samples numbers 1, 5, 9, 13 will be used for illustrative purposes. The thermal conductivity of these samples and their associated error bars are shown in Fig. 3.

An analysis of variances (ANOVA) [25] is carried out for the different experiments on a given sample. The results of the ANOVA for sample # 13 is shown in the Table I. Each run consists of 9 temperature values between 273 K and 473 K. The ANOVA results for the other samples can be found in Table IV in Appendix A.

Based on the sum squared errors for the different treatments, it is concluded that there is little variation within the experiments. This is to be expected since the corresponding values of the different experiments are within ± 1 K of the set-point temperature. In contrast, there is a large variation in each treatment since the values within each experiment are at different conditions.

There are two degrees of freedom for the treatments since there are three runs and twenty-four degrees of freedom for the individual readings within each experiment. The F-statistic is found to be 0.54989 which is less that the value (1.47) found from the F-statistic tables [25]. The hypothesis in the ANOVA is that the means of different experiments are the same. This claim is true if the computed F-statistic is less than the critical F-statistic. Thus, the ANOVA results show that the mean of each of the three experiments on sample # 13 is the same.

The F-test provides no information about the variance of the data. To estimate the bounds on the data, a χ-squared test is conducted on different experiments of the same sample at each temperature point, which provides a bound for the data at each temperature point. Using

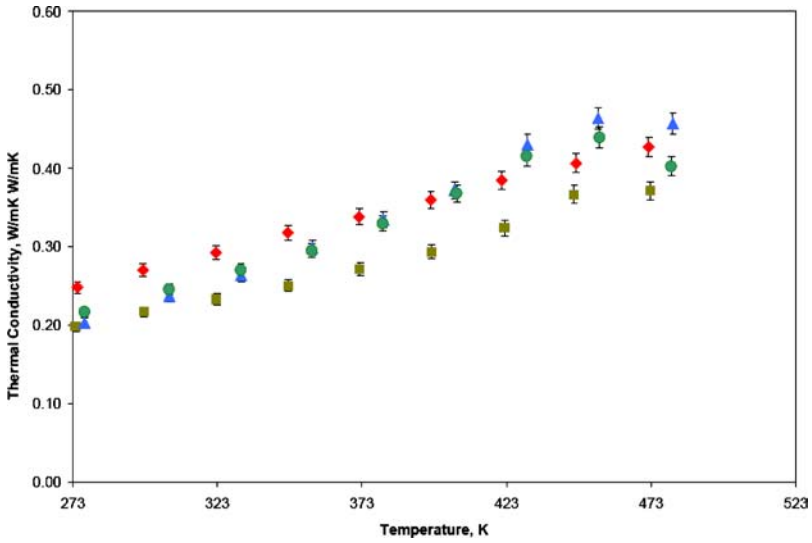

Figure 3 Thermal conductivity of example samples.

the results of the χ-squared test a confidence interval is constructed for a given sample over the temperature range of interest. Fig. 4 shows the thermal conductivity for the entire temperatures range along with the uncertainty and the 95% confidence interval.

4.2. Model predictions

The values of the thermal conductivities of the constituents, i.e. APO-BMI resin and carbon are required to calculate thermal conductivity of the foam. However, it is not possible to prepare a solid piece of APO-BMI because of out-gassing of the resin during curing. Hence, the value of 0.307 W $m^{-1}K^{-1}$, taken from the open literature for maleimides is used [26] . Additionally, accurate measurements of the thermal conductivity of the phenolic carbon powder are not obtainable due to equipment availability. To overcome this, the thermal conductivity value of phenolic carbon at 298 K, 4.6 W $m^{-1}K^{-1}$, is used [28].

Fig. 5 compares the models' prediction of thermal conductivity to the experimental data. The results indicate that: (1) the predictions are quite reasonable at lower temperatures for all foams; (2) at higher temperatures, only the Eucken model gives satisfactory predictions of the thermal conductivity; and (3) based on the relative error (see Table V), the Eucken model gave the best predictions followed by the Cheng-Vachon model, and then the foam model.

The foam model was proposed for two-phase foams. It however, does not account for the internal structure of the foam. Similarly, the Cheng-Vachon model is based on a resistance-in-series model and considers the discontinuous phase to be distributed parabolically in the foam. Thus, it too does not account for the internal structure. This lack of accounting for the internal structure may be the reason for the relatively poor performance of these two

TABLE I. ANOVA of Samples # 1, 5, 9, 13

Sample #	Source	Sum squares	DOF	Variance	F-stat
1	Treatments	0.00009	2	0.00045	0.09443
	Error	0.01101	24	0.00004	–
	Total	0.01100	26	–	–
5	Treatments	0.00048	2	0.00114	0.21813
	Error	0.02660	24	0.00024	–
	Total	0.02705	26	–	–
9	Treatments	0.00044	2	0.00022	0.09861
	Error	0.08528	24	0.00021	–
	Total	0.05327	26	–	–
13	Treatments	0.00375	2	0.00314	0.54989
	Error	0.08192	24	0.00188	–
	Total	0.08567	26	–	–

TABLE II. Errors (%) for the different models for sample #1

Temperature K	Thermal conductivity W/m-K	Percentage error			Model predictions		
		Cheng-Vachon	Eucken	Leach	Cheng-Vachon	Eucken	Leach
273	0.248	9.67	−2.16	5.21	0.224	0.254	0.251
323	0.292	16.74	5.29	12.99	0.243	0.277	0.274
373	0.338	22.65	11.63	19.47	0.261	0.299	0.295
423	0.385	27.58	17.00	24.88	0.279	0.309	0.316

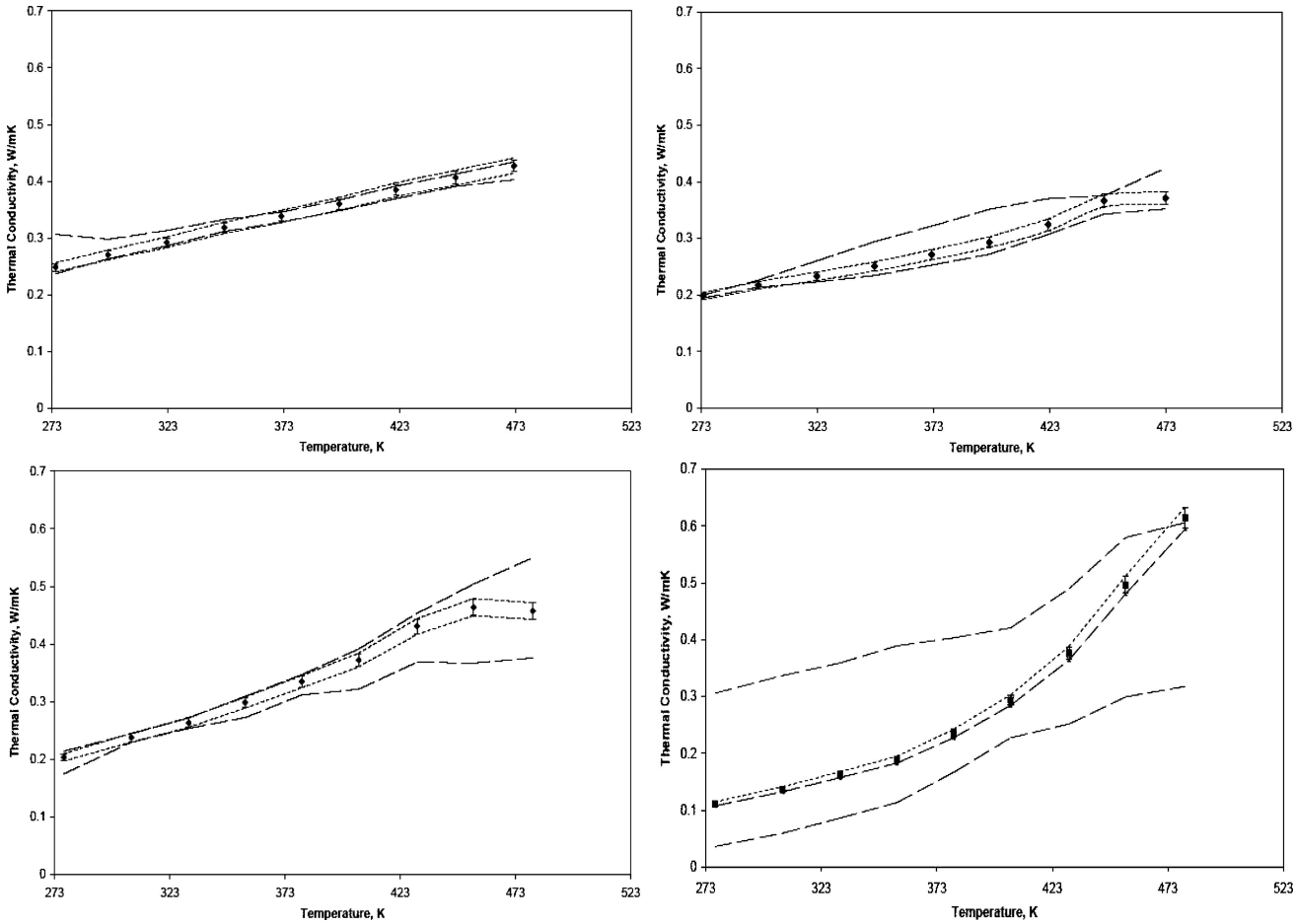

Figure 4 Thermal conductivity.

models (foam model and the Cheng-Vachon model), especially at higher temperatures. The Eucken model, based on self-consistent field theory, was originally proposed for solid composites. One possible source of error in the predictions of the Eucken model is that the air-voids may not necessarily remain spherical during formation of the foam but may become elongated and create a greater resistance to heat flow in the longitudinal direction.

In addition, the model used to estimate the contribution due to the radiation has been developed for high porosity, low density foams whereas the foams studied in this work are comparatively higher density and low porosity. Therefore, there errors in the model predictions at higher temperatures might also be due errors in calculating the effective thermal conductivity due to radiation (k_r).

5. Summary

In this work, the thermal conductivity of three-phase syntactic foams with phenolic-based carbon microspheres as a filler and amorphous bismaleimide (APO-BMI) resin as a binder was measured experimentally using a guarded heat flow meter. This work represents the first attempt to measure and model the thermal conductivity of three-phase syntactic foams. A statistical analysis of the experimental data supported the repeatability and thus the efficacy of a guarded heat flow meter to measure the thermal conductivity of low conductive materials accurately [2]. The tap density and the relative amount of the filler (carbon microballoons) in the foam were identified as parameters that can be manipulated to control the thermal properties of the foams.

The experimental thermal conductivity data were compared to the predictions of three well accepted models. It was found that all the models used provided satisfactory predictions at lower temperatures. The Eucken model provided the best estimates of the three models chosen for comparison, with errors ranging from ± 0.04 % at low temperatures to $\pm 35\%$ at higher temperatures. A sensitivity study showed that the thermal conductivity of the foam is a strong function of the thermal conductivity of the carbon that is used in the manufacture of the phenolic-based carbon microspheres. This suggests that the thermal conductivity of the carbon itself needs to be characterized more accurately to better predict the thermal conductivity of three-phase foams.

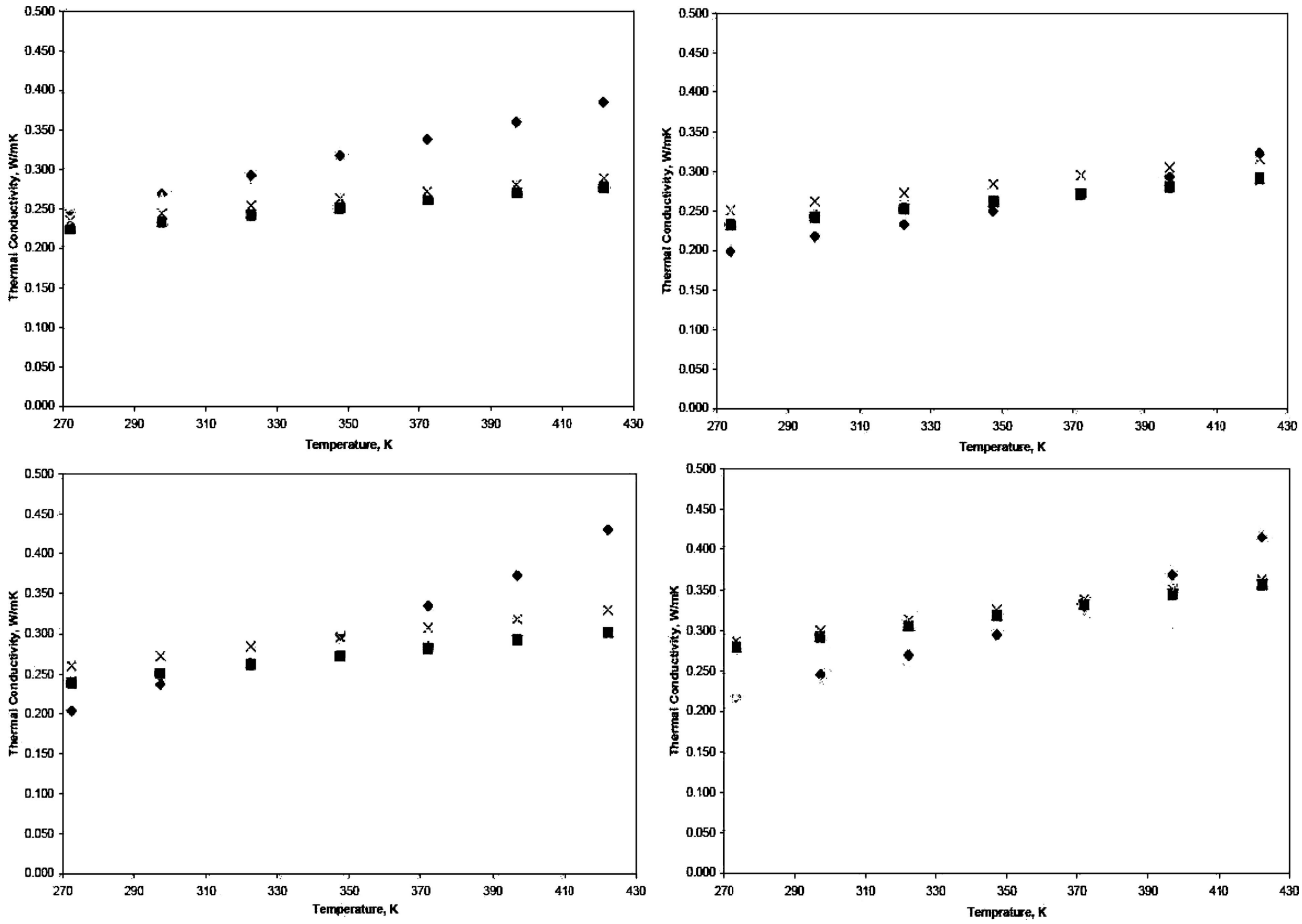

Figure 5 Model predictions of thermal conductivity.

Nomenclature

β	Extinction coefficient, m^{-1}
δQ	The error in measurement of heat flow, W
δT	The error in measurement of temperature, K
δt	The error in measurement of sample thickness, mm
B	A parameter in the Cheng-Vachon equation, function of v_d
C	A parameter in the Cheng-Vachon equation, function of v_d
k_a	Thermal conductivity of air, W $m^{-1}K^{-1}$
k_{cmb}	Thermal conductivity of the carbon microspheres, W $m^{-1}K^{-1}$
k_d	Thermal conductivity of the discontinuous phase, W $m^{-1}K^{-1}$
k_{solid}	Thermal conductivity of the solid phase, W $m^{-1}K^{-1}$
k_{teflon}	Thermal conductivity of teflon, W $m^{-1}K^{-1}$
Q_1	Ratio of the thermal conductivity of continuous phase to the discontinuous phase
Q_{edge}	Edge heat loss, W
q_r	Radiative heat flux, W m^{-2}
R_s	Thermal resistance, m^2 K W^{-1}
R_e	Thermal resistance per unit thickness of the sample, m K W^{-1}
T	Temperature, K
t_{teflon}	Thickness of teflon insulation between sample and guard heater, m
v_a	Volume fraction of air
v_d	Volume fraction of the discontinuous phase
q	Heat flux across the sample, W m^{-2}
z	Thickness of the sample, m
ρ_f	Density of the foam, kg m^{-3}
σ	Stefan-Boltzmann constant, W $m^{-2}K^{-4}$
τ_0	Optical thickness
k	Thermal conductivity, W $m^{-1}K^{-1}$
k_r	Radiative thermal conductivity, $Wm^{-1}K^{-1}$
k_{tot}	Total effective thermal conductivity the sample, W m^{-2}
Q	The total heat flowing from the heater plate to the upper plate, W
Q_{meas}	The heat measured by the heat transducer in the heat flow meter, W
q_{tot}	Total heat flux flowing through the sample, W m^{-2}
t	Actual thickness, m
q	Conductive heat flux flowing through the sample, W m^{-2}

Appendix A: Sample properties and model predictions

TABLE III. The specifications of the samples used in the experiment

Sample #	Thickness (cm)	Diameter (cm)	Mass (g)	Foam Density (g/cc)	Tap Density (g/cc)	Carbon Microballoon volume fraction
1	0.632	5.460	5.0800	0.343	0.1969	0.656
2	0.636	5.466	5.0840	0.342	0.1969	0.653
3	0.677	5.473	5.3100	0.334	0.1611	0.588
4	0.636	5.479	5.4027	0.360	0.2148	0.697
5	0.636	5.460	5.0813	0.341	0.1620	0.595
6	0.632	5.466	5.0839	0.343	0.1782	0.603
7	0.642	5.473	5.3122	0.350	0.1944	0.646
8	0.636	5.479	5.4027	0.360	0.2106	0.632
9	0.646	5.464	4.5851	0.303	0.1540	0.599
10	0.642	5.468	4.5887	0.304	0.1694	0.648
11	0.640	5.469	4.6536	0.308	0.1848	0.594
12	0.643	5.471	4.9611	0.328	0.2002	0.655
13	0.644	5.250	4.9900	0.358	0.1450	0.685
14	0.642	5.465	5.0519	0.335	0.1595	0.680
15	0.640	5.465	4.9696	0.331	0.1740	0.625
16	0.635	5.467	4.7475	0.318	0.1885	0.581
Average	0.642	5.455	5.0180	0.335	0.1806	0.634
Std deviation	0.011	0.055	0.2688	0.019	0.0209	0.037
Variance	0.0001	0.003	0.072	0.001	0.0004	0.001

TABLE IV. Analysis of variances

Sample #	Source	Sum squared	DOF	Variance	F-stat	Sample #	Source	Sum squared	DOF	Variance	F-stat
2	Treatments	0.00008	2	0.00002	0.05041	10	Treatments	0.00475	2	0.00234	1.1422
	Error	0.01311	24	0.00054	–		Error	0.04987	24	0.00217	–
	Total	0.01320	26	–	–		Total	0.0546	26	–	–
3	Treatments	0.00001	2	0.00005	0.01412	11	Treatments	0.00617	2	0.00303	0.93899
	Error	0.0089	24	0.00037	–		Error	0.07879	24	0.00328	–
	Total	0.0091	26	–	–		Total	0.08501	26	–	–
4	Treatments	0.00092	2	0.00046	0.59486	12	Treatments	0.0180	2	0.00897	0.42128
	Error	0.01857	24	0.00077	–		Error	0.51262	24	0.02136	–
	Total	0.01950	26	–	–		Total	0.08567	26	–	–
6	Treatments	0.00082	2	0.00041	0.40912	14	Treatments	0.00240	2	0.00121	0.78255
	Error	0.0241	24	0.00117	–		Error	0.03677	24	0.00152	–
	Total	0.0249	26	–	–		Total	0.03916	26	–	–
7	Treatments	0.00009	2	0.00005	0.04392	15	Treatments	0.00259	2	0.00128	1.01246
	Error	0.0238	24	0.00101	–		Error	0.03067	24	0.00129	–
	Total	0.0239	26	–	–		Total	0.0332	26	–	–
8	Treatments	0.00007	2	0.00036	0.38506	16	Treatments	0.00032	2	0.00016	0.25557
	Error	0.0225	24	0.00094	–		Error	0.01500	24	0.00062	–
	Total	0.0232	26	–	–		Total	0.01531	26	–	–

TABLE V. Percentage errors for the different models for samples 2 to 16

Sample #	Temperature K	Thermal Conductivity W/m-K	Percentage error			Model predictions		
			Cheng-Vachon	Eucken	Leach	Cheng-Vachon	Eucken	Leach
2	273	0.275	−8.46	−30.20	−17.02	0.234	0.281	0.253
	323	0.303	4.30	−15.89	−3.62	0.255	0.308	0.276
	373	0.340	16.20	−2.18	9.03	0.275	0.335	0.298
	423	0.384	30.00	14.18	23.88	0.295	0.361	0.321

TABLE V. Percentage errors for the different models for samples 2 to 16

Sample #	Temperature K	Thermal Conductivity W/m-K	Percentage error			Model predictions		
			Cheng-Vachon	Eucken	Leach	Cheng-Vachon	Eucken	Leach
3	273	0.216	−8.41	−30.13	−16.97	0.232	0.281	0.253
	323	0.253	−0.50	−21.71	−8.84	0.260	0.308	0.276
	373	0.334	17.75	−0.31	10.69	0.282	0.335	0.298
	423	0.379	22.29	4.69	15.47	0.302	0.361	0.320
4	273	0.211	−11.04	−33.30	−19.82	0.224	0.281	0.253
	323	0.263	3.05	−17.42	−5.00	0.254	0.308	0.276
	373	0.319	13.71	−5.23	6.31	0.277	0.335	0.298
	423	0.374	21.12	3.26	14.20	0.291	0.361	0.321
5	273	0.198	−17.67	−41.07	−26.94	0.233	0.279	0.251
	323	0.233	−8.47	−31.11	−17.43	0.253	0.306	0.274
	373	0.271	−0.29	−22.01	−8.85	0.272	0.331	0.295
	423	0.324	10.17	−9.83	2.34	0.291	0.356	0.316
6	273	0.216	−8.46	−30.20	−17.02	0.234	0.281	0.253
	323	0.266	4.30	−15.89	−3.62	0.255	0.308	0.276
	373	0.328	16.20	−2.18	9.03	0.275	0.335	0.298
	423	0.421	30.00	14.18	23.88	0.295	0.361	0.321
7	273	0.216	−6.09	−28.27	−18.82	0.229	0.277	0.257
	323	0.253	−2.08	−19.96	−5.78	0.259	0.304	0.268
	373	0.334	18.74	−0.31	12.05	0.271	0.335	0.294
	423	0.379	19.65	3.20	15.47	0.305	0.367	0.320
8	273	0.211	−5.35	−4.85	−10.33	0.222	0.221	0.233
	323	0.263	3.24	−2.19	−5.00	0.254	0.268	0.276
	373	0.319	12.52	−5.23	−12.53	0.279	0.335	0.358
	423	0.374	3.17	3.26	14.20	0.362	0.361	0.321
9	273	0.203	−18.15	−32.89	−27.88	0.240	0.270	0.260
	323	0.264	0.77	−12.18	−7.79	0.262	0.296	0.284
	373	0.335	15.70	4.35	8.21	0.282	0.320	0.307
	423	0.430	29.77	20.10	23.41	0.302	0.344	0.330
10	273	0.222	−15.92	−22.58	−17.86	0.258	0.272	0.262
	323	0.284	0.78	−5.12	−0.91	0.281	0.298	0.286
	373	0.367	16.97	11.94	15.57	0.304	0.323	0.309
	423	0.421	22.32	17.57	21.06	0.327	0.347	0.332
11	273	0.209	−18.52	−20.81	−10.74	0.248	0.252	0.231
	323	0.266	−2.10	−7.27	−7.67	0.271	0.285	0.286
	373	0.336	9.35	3.85	7.82	0.304	0.323	0.309
	423	0.372	6.73	6.74	10.68	0.347	0.347	0.332
12	273	0.215	−19.62	−12.52	−9.40	0.257	0.242	0.235
	323	0.298	5.57	−0.04	3.96	0.281	0.298	0.286
	373	0.372	7.38	13.17	16.76	0.344	0.323	0.309
	423	0.467	15.09	17.23	20.37	0.397	0.387	0.372
13	273	0.203	−18.15	−32.89	−50.81	0.240	0.270	0.307
	323	0.264	0.77	−12.18	−23.87	0.262	0.296	0.327
	373	0.335	15.70	4.35	−3.51	0.282	0.320	0.346
	423	0.430	29.77	20.10	14.83	0.302	0.344	0.366
14	273	0.211	−32.82	−4.60	−36.61	0.280	0.221	0.288
	323	0.265	−15.46	4.79	−18.11	0.306	0.253	0.313
	373	0.325	−2.30	12.46	−4.17	0.332	0.284	0.338
	423	0.341	−1.05	12.18	−2.68	0.345	0.300	0.350
15	273	0.220	5.17	0.24	5.77	0.208	0.219	0.207
	323	0.248	0.78	−0.94	−25.43	0.246	0.251	0.311
	373	0.369	6.42	20.23	7.33	0.345	0.294	0.342
	423	0.488	16.24	14.94	19.56	0.409	0.415	0.393
16	273	0.223	6.16	1.53	2.56	0.209	0.220	0.217
	323	0.285	−7.56	4.28	−10.03	0.306	0.273	0.313
	373	0.359	4.77	18.95	5.87	0.342	0.291	0.338
	423	0.411	12.91	8.59	11.67	0.358	0.375	0.363

TABLE VI. Thermal conductivity of all samples in the temperature range 0-200K

	Thermal conductivity, $Wm^{-1}K^{-1}$								
Temperature, K	273	298	323	348	373	398	423	448	473
Sample #									
1	0.2483	0.2702	0.2924	0.3181	0.3380	0.3599	0.3599	0.4064	0.4273
1	0.2752	0.2840	0.3032	0.3257	0.3403	0.3610	0.3610	0.4053	0.4217
3	0.1988	0.2220	0.2417	0.2623	0.2751	0.2927	0.2927	0.3275	0.3405
4	0.2798	0.2971	0.3182	0.3403	0.3592	0.3828	0.3828	0.4373	0.4608
5	0.1963	0.2219	0.2460	0.2708	0.2956	0.3208	0.3208	0.3709	0.3965
6	0.2161	0.2411	0.2662	0.2956	0.3280	0.3696	0.3208	0.4211	0.4517
7	0.2160	0.2523	0.2534	0.2708	0.3340	0.3464	0.3464	0.4273	0.4393
8	0.2109	0.2360	0.2627	0.2918	0.3186	0.3455	0.3455	0.4012	0.4292
9	0.2033	0.2374	0.2637	0.2932	0.3347	0.3723	0.3723	0.4638	0.4573
10	0.2223	0.2504	0.2836	0.2985	0.3665	0.3834	0.3834	0.4926	0.4423
11	0.2089	0.2375	0.2658	0.3212	0.3357	0.3497	0.3497	0.4990	0.6281
12	0.2149	0.2575	0.2979	0.2984	0.3717	0.4549	0.4549	0.4988	0.5433
13	0.1109	0.1367	0.1624	0.3120	0.2349	0.2938	0.2938	0.4962	0.6144
14	0.1234	0.1563	0.1854	0.1888	0.2464	0.3072	0.3072	0.4509	0.3806
15	0.2158	0.2482	0.2895	0.2142	0.3689	0.3862	0.3862	0.5138	0.5175
16	0.2469	0.2566	0.2872	0.3409	0.3270	0.3378	0.3378	0.3747	0.3997

Appendix B: Uncertainty analysis

Since, the uncertainty value is not fixed, it may be treated as a statistical variable. The sources of uncertainty in the measurement include:

1. Uncertainty in the heat flow through the sample.
The heat flux transducer is located below the sample. Thus, what is measured is the heat that is being transferred to the sample from the lower heater. This heat may not be the actual heat that passes through the sample as there may be losses. The losses may be due to contact resistance, radial losses, etc.

(a) Heat loss due to contact resistance: When heat is transferred from the heater to the sample, there may be some losses due to improper contact between the surface of the heater and the sample surface. Thus, errors in the heat flux passing through the sample may exist. To reduce these losses, a Dow-Corning© heat sink compound is applied to the surfaces of the sample in contact with the heaters (top and bottom).

(b) Edge losses: There may be heat losses from the sample to the guard heater in spite of the presence of a teflon ring around the sample. Ideally, the temperature of the sample and that of the guard heater are equal. In practice they are not, due to radial heat losses across the guard ring. These radial losses are similar to radial flow across a cylinder and the following formula may be used to estimate the heat lost to the guard ring.

$$Q_{\text{edge}} = \frac{2\pi k_{\text{teflon}} t_{\text{teflon}} \Delta T}{ln(r_2/r_1)}$$

where Q_{edge} is the heat loss to be calculated, k_{teflon} is the thermal conductivity of the insulation between the sample and the guard heater, t_{teflon} is the thickness of the insulation, ΔT is the temperature difference between the sample and the guard heater, while r_2 and r_1 are the outer and inner radii, respectively of the teflon ring.

2. The thickness of the sample is measured using a pair of digital Vernier callipers. The least count of this instrument is 0.01 mm. Thus, the errors in the measurement of the thickness and diameter of the sample are ± 0.01 mm. This error is propagated in the measurement of the cross-sectional area and the volume of the sample. The foam density measurement therefore has an error of ± 1.

3. Errors in the measurement of the heat-flux.
The transducer that measures the heat flux through the sample may introduce some error. In previous studies by [13], the measurement errors have been estimated to be ± 3.

4. Errors in the temperature measurements. The thermocouples used to measure the temperature of the sample cannot be calibrated individually. Errors associated with this are assumed to be of the order of ± 1 K.

The total uncertainty in the measurement of power is given by [24],

$$\frac{\delta Q}{Q} = \sqrt{\frac{\delta Q_{\text{edge}}^2 + \delta Q_{\text{meas}}^2}{Q^2}}. \quad (13)$$

The total uncertainty in the measurement of the thermal conductivity is the root mean squared sum of these uncertainties,

$$\frac{\delta k_{\text{eff}}}{k_{\text{eff}}} = \sqrt{\left(\frac{\delta Q}{Q}\right)^2 + \left(\frac{\delta t}{t}\right)^2 + \left(\frac{\delta T}{T}\right)^2} \qquad (14)$$

where Q is the power, t is the thickness, and T is the temperature.

References

1. K. ASHIDA, Syntactic foams. "Handbook of Plastic Foams: Types, Properties, Manufacture and Applications" (Noyes Publications, Park Ridge, NJ, 1995) p. 147.
2. S. KLARSFELD, Guarded hot plate method for thermal conductivity measurements. "Compendium of Thermophysical Property Measurement Methods: Survey of Measurement Techniques" (Plenum Press, New York, NY, 1984) Vol. 1, p. 169.
3. Operation and Maintainence Manual, TCA-200-LT-A Guarded Heat Flow Meter (Bedford, MA).
4. A. G. LEACH, Thermal conductivity of foams-I: Models for heat conduction. *Journal of Physics D: Applied Physics* **26** (1993) 733–739.
5. L GLICKSMAN, M. SCHUETZ and M. SINOFSKY, Radiation heat transfer in foam insulation. *International Journal of Heat and Mass Transfer* **30** (1987) 187–197.
6. J. D. FELSKE, Effective thermal conductivity of composite spheres in a continuous medium with contact resistance. *Ibid.* **47** (2004) 3453–3461.
7. Z. HASHIN, Assessment of self consistent scheme approximation: Conductivity of particulate composites. *Journal of Composite Materials* **2** (1968) 284–300.
8. Y. BENVENISTE and T. MILOH, Effective conductivity of composites with imperfect contact at the constituent interfaces. *International Journal of Engineering Science* **24** (1986) 1537–1552.
9. V. S. SHABDE, Experimental determination of the thermal conductivity of syntactic foams. Technical report, TTU, Department of Chemical Engineering, Lubbock, TX, 2005.
10. Y. AGARI and T. UNO, Estimation of thermal conductivities of filled polymers. *Journal of Applied Polymer Science* **32** (1986) 5705–5712.
11. S. C. CHENG and R. I. VACHON, The prediction of the thermal conductivity of two and three phase solid heterogenous mixtures. *International Journal of Heat and Mass Transfer* **12** (1968) 249–264.
12. C. MAXWELL, "A Treastise on Electricity and Magnetism" (Clarendon Press, Oxford, 1892).
13. C. Y. ZHAO, T. J. LU, H. P. HODSON, and J. D. JACKSON, The temperature dependence of effective thermal conductivity of open-celled steel alloy foams. *Material Science and Engineering A* **367** (2004) 123–131.
14. D. DOERMANN and J. F. SCADURA, Heat transfer in open cell foam insulation. *Journal of Heat Transfer* (1996) 83–93.
15. H. C. HOTTEL and A. F. SAROFIM, "Radiative Transfer" (McGraw-Hill, New York, NY, 4th edition, 1967).
16. W. TAO, H. HSU, C. CHANG, C. HSU, and Y. LIN, Measurement and prediction of thermal conductivity of open-cell rigid polyurethane foam. *Journal of cellular Plastics* **37** (2001) 310–331.
17. M. KYO, T. KATOH, T. KASHIWAGA, and Y. KAMATA, Effective thermal conductivity of composite foam. *Heat Transfer: Japanese Research* **23** (1994) 258–276.
18. A. G. LEACH, Thermal conductivity of foams-II: The thermal conductivity of a layer mineral foam. *Journal of Physics D: Applied Physics* **26** (1993) 740–745.
19. R. TSUKUDA, S. SUMIMOTO, and T. OZAWA, Thermal conductivity and heat capacity of abs resin composites. *Journal of Applied Polymer Science* **63** (1997) 1279–1286.
20. O. ALMANZA, M. A. RODRÍGUEZ-PÉREZ, and J. A. SAJA, Applicability of the transient plane source method to measure thermal conductivity of low-density polyethylene foams. *Journal of Polymer Science* **42** (2004) 1226–1234.
21. W. R. DAVIS, Hotwire method of measurement of thermal conductivity of refractory materials. "Compendium of Thermophysical Property Measurement Methods Survey of Measurement Techniques" (Plenum Press, New York, NY, 1984) Vol. 1, pp. 231–254.
22. A. Z. ZINCHENKO, Effective conductivity of loaded granular materials by numerical simulation. *Philosophical Transactions of the Royal Society of London* **356** (1997) 2953–2998.
23. A. EUCKEN, Thermal conductivity of ceramic refractory materials; calculation from thermal conductivity of constituents. *Ceramic Abstracts* **11** (1932).
24. S. J. KLINE, The purposes of uncertainty analysis. *Journal of Fluids Engineering* **107** (1985) 153–160.
25. L. R. OTT and M. LONGNECKER, "Statistical Methods and Data Analysis" (Duxbury, CA, 5th edition, 2001).
26. C. RESEWSKI and W. BUCHGRABER, Properties of new polyimide foams and polyimide foam filled honeycomb composites. *Materials Science and Engineering Technology* **34** (2003) 365–369.
27. S. C. CHENG and R. I. VACHON, A technique for predicting the thermal conductivity of suspensions, emulsions and porous materials. *International Journal of Heat and Mass Transfer* **13** (1969) 537–546.
28. H. O. PIERSON, "Handbook of Carbon, Graphite, Diamond and Fullerenes—Properties, Processing and Applications" (New York, NY, 1st edition, 1993).